

REPORT DOCUMENTATION PAGE

The public reporting burden for this collection of information is estimated to average 1 hour per response, including the time for reviewing instructions, searching existing data sources, gathering and maintaining the data needed, and completing and reviewing the collection of information. Send comments regarding this burden estimate or any other aspect of this collection of information, including suggestions for reducing the burden, to the Department of Defense, Executive Service Directorate (0704-0188). Respondents should be aware that notwithstanding any other provision of law, no person shall be subject to any penalty for failing to comply with a collection of information if it does not display a currently valid OMB control number.

PLEASE DO NOT RETURN YOUR FORM TO THE ABOVE ORGANIZATION.

1. REPORT DATE (DD-MM-YYYY) 03-01-2009		2. REPORT TYPE Final Report		3. DATES COVERED (From - To) From 01-12-2005 to 30-11-2008	
4. TITLE AND SUBTITLE The Chemical Dynamics of State-Selected Atomic and Diatomic Ions of Aerospace Relevance				5a. CONTRACT NUMBER FA9550-06-1-0073	
				5b. GRANT NUMBER	
				5c. PROGRAM ELEMENT NUMBER	
6. AUTHOR(S) Cheuk-Yiu Ng				5d. PROJECT NUMBER	
				5e. TASK NUMBER	
				5f. WORK UNIT NUMBER	
7. PERFORMING ORGANIZATION NAME(S) AND ADDRESS(ES) University of California, Davis One Shields Avenue, Davis, CA 95616				8. PERFORMING ORGANIZATION REPORT NUMBER	
9. SPONSORING/MONITORING AGENCY NAME(S) AND ADDRESS(ES) Air Force Office for Scientific Research AFOSR/NA 875 N. Randolph St. Suite 325, Room 3112 Arlington, VA 22203				10. SPONSOR/MONITOR'S ACRONYM(S) AFOSR/NA	
				11. SPONSOR/MONITOR'S REPORT NUMBER(S)	
12. DISTRIBUTION/AVAILABILITY STATEMENT Approved for public release					
13. SUPPLEMENTARY NOTES					
14. ABSTRACT Elastic scattering between xenon ions and xenon atoms can produce ion currents at large angles with respect to the axis of electrostatic thruster, and thus, can cause significant material erosion due to sputtering. Guided-ion beam differential cross sections have been measured for Xe++Xe and Xe2++Xe at laboratory ion energies between 5 and 40 eV per ion charge. For this singly charged system, the experimental absolute differential cross sections are found to be in excellent agreement with classical elastic scattering calculations based on the most accurate ab initio ion-atom interaction potentials. The measurements for the doubly charged system are used to derive an approximate effective Xe2++Xe interaction potential. These potentials are used to calculate absolute differential cross sections for both ion charge states at a typical Hall thruster ion energy of 300 eV per unit charge. The importance of Xe2+ with respect to material erosion is discussed. It is concluded that at typical charge-state ratios, doubly charged ions only have an impact at elastic scattering angles where the scattered ion energy in the laboratory (thruster) frame of reference is low and the sputtering yields depend very strongly in kinetic energy.					
15. SUBJECT TERMS Ion thruster; material erosion					
16. SECURITY CLASSIFICATION OF:			17. LIMITATION OF ABSTRACT	18. NUMBER OF PAGES	19a. NAME OF RESPONSIBLE PERSON
a. REPORT	b. ABSTRACT	c. THIS PAGE			Cheuk-Yiu Ng
UU			UU	21	19b. TELEPHONE NUMBER (Include area code) 530-754-9645

FINAL AFOSR REPORT (Dec. 1, 2005-Nov. 30, 2008)

I. Grant Title:

The Chemical Dynamics of State-Selected Atomic and Diatomic Ions of Aerospace Relevance

II. Principal Investigator and Address

Cheuk-Yiu Ng

Address: Department of Chemistry
University of California at Davis
Davis, California 95616

III. Contract Number: FA9550-06-1-0073

20090324152

IV. Objective:

The main goal of the previous project was to determine absolute state-selected integral cross-sections for reactions between atmospheric diatomic ions and the rare gas atoms, with an emphasis on the reactions of reactant ions in highly vibrationally excited states. These state-selected absolute total cross section measurements are needed for improving the Direct Simulation Monte Carlo and Particles in Cell methods, which have been used for modeling the chemistry occurring in non-equilibrium aerospace environments of interest to the Air Force (such as the hypersonic air plasma associated with communications blackouts of reentry space vehicles and the plasmas of electric propulsion thrusters).

V. Published results and scientific and technical developments

V.1. Refereed publications acknowledging the support of this AFOSR grant (2006-present)

1. M.-K. Bahng, X. Xing, S.-J. Baek, X.-M. Qian, and C. Y. Ng, "A combined VUV synchrotron pulsed field ionization-photoelectron and IR-VUV laser photoion depletion study of ammonia", *J. Phys. Chem. A*, **110**, 8488-8496 (2006).
2. J. Zhou, K.-C. Lau, E. Hassanein, H.-F. Xu, S.-X. Tian, B. Jones, and C. Y. Ng, "A photodissociation study of CH₂BrCl in the A-band using the time-sliced velocity ion imaging method", *J. Chem. Phys.* **124**, 034309 (2006).
3. K.-C. Lau and C. Y. Ng, "Accurate *ab initio* predictions of ionization energies and heats of formation for the 2-C₃H₇, C₆H₅, and C₇H₇ radicals", *J. Chem. Phys.* **124**, 044323 (2006).
4. P. Wang, H. K. Woo, K. C. Lau, X. Xing, C. Y. Ng, A. S. Zyubin, and A. M. Mebel, "Infrared vibrational spectroscopy of *cis*-dichloroethene in Rydberg states", *J. Chem. Phys.* **124**, 064310 (2006) (Selected as the March 2006 issue of Virtual Journal of Ultrafast Science).
5. T. Zhang, X. N. Tang, K.-C. Lau, C. Y. Ng, C. Nicolas, D. S. Peterka, M. Ahmed, M. L. Morton, B. Ruscic, R. Yang, L. X. Wei, C. Q. Huang, B. Yang, J. Wang, L. S. Sheng, Y. W. Zhang, and F. Qi, "Direct identification of propargyl radical in combustion flames by VUV photoionization mass spectrometry", *J. Chem. Phys.* **124**, 074302 (2006).
6. K.-C. Lau and C. Y. Ng, "Accurate *ab initio* predictions of ionization energies and heats of formation for the cyclopropenylidene, propargylene and propadienylidene radicals", *Chinese Journal of Chemical Physics* (invited article), **19**, 29-38 (2006).

7. K. C. Lau, H. K. Woo, P. Wang, X. Xing, and C. Y. Ng, "Vacuum ultraviolet laser pulsed field ionization-photoelectron study of *cis*-dichloroethene", *J. Chem. Phys.* **124**, 224311 (2006).
8. R.A. Dressler, Y. Chiu, D. Levandier, X. N. Tang, Y. Hou, C. Chang, C. Houchins, H. Xu, and C. Y. Ng, "The Study of State-Selected Ion-Molecule Reactions using the Pulsed-Field Ionization-Photoion Technique", *J. Chem. Phys.* (invited article for the special issue on Chemical Dynamics), **125**, 132306 (2006).
9. X. Xing, M.-K. Bahng, P. Wang, K. C. Lau, S.-J. Baek, and C. Y. Ng, "Rovibrationally selected and resolved state-to-state photoionization of ethylene using the infrared-vacuum ultraviolet pulsed field ionization-photoelectron method", *J. Chem. Phys.* **125**, 1333304 (2006).
10. C.Y. Ng, "Introduction: Chemical Dynamics", *J. Chem. Phys.* **125**, 132201 (2006).
11. K.-C. Lau and C.-Y. Ng, "Benchmarking state-of-the-art *ab initio* thermochemical predictions with accurate pulsed-field ionization photoion-photoelectron measurements", *Accounts on Chemical Research*, **39**, 823-829 (2006).
12. S. Stimson, M. Evans, C.-W. Hsu, and C. Y. Ng, "Rotationally Resolved Vacuum Ultraviolet Pulsed Field Ionization-Photoelectron Bands for $\text{HD}^+(\chi^2\Sigma_g^+, v^+=0-20)$ ", *J. Chem. Phys.* **126**, 164303 (2007).
13. X. Xing, B. Reed, K.-C. Lau, C. Y. Ng, X. Zhang, G. B. Ellison, "Vacuum ultraviolet laser pulsed field ionization-photoelectron study of allyl radical CH_2CHCH_2 ", *J. Chem. Phys.* (communication), **126**, 171101 (2007).
14. J. Li, J. Yang, Y. Mo, K.-C. Lau, and C. Y. Ng, "A combined vacuum ultraviolet laser and synchrotron pulsed field ionization study of CH_2BrCl ", *J. Chem. Phys.* **126**, 184304 (2007). Selected for the May 28, 2007 issue of Virtual Journal of Nanoscale Science & Technology.
15. X. N. Tang, H. F. Xu, C. Houchins, C. Y. Ng, Y. Chiu, R. A. Dressler, and D. J. Levandier. "An experimental and quasi-classical trajectory study of the rovibrationally state-selected reactions: $\text{HD}^+(v=0-15, j=1) + \text{He} \rightarrow \text{HeH}^+(\text{HeD}^+) + \text{D(H)}$ ", *J. Chem. Phys.* **126**, 234305 (2007).
16. X. Xing, B. Reed, K.-C. Lau, C. S. Lam, and C. Y. Ng, "Assignment of rovibrational transitions of propyne in the region of $2934\text{-}2952\text{ cm}^{-1}$ measured by the two-color IR-VUV laser Photoion and Photoelectron methods", *J. Chem. Phys.* **127**, 044313 (2007).
17. C. Chang, C. Y. Ng, S. Stimson, M. Evans, and C.-W. Hsu, "Rotationally Resolved Pulsed Field Ionization-Photoelectron Bands of $\text{H}_2^+(\chi^2\Sigma_g^+, v^+=0-18)$ ", *Chinese J. Chem. Phys.* **20**, 352 (2007).

18. X. N. Tang, C. Houchins, K.-C. Lau, C. Y. Ng, R. A. Dressler, Y.H. Chiu, T.-S. Chu, and K.-L. Han, "A time-dependent wave packet quantum scattering study of the reaction $\text{HD}^+(\nu=0-3; j=1) + \text{He} \rightarrow \text{HeH}^+(\text{HeD}^+) + \text{D}(\text{H})$ ", *J. Chem. Phys.* **127**, 164318 (2007).
19. J. Zhou, B. Jones, X. Yang, W. M. Jackson, and C. Y. Ng, "A vacuum ultraviolet laser photoionization and pulsed field ionization study of nascent $\text{S}(^3P_{2,1,0}; ^1D_2)$ formed in the 193.3 nm photodissociation of CS_2 ", *J. Chem. Phys.* **128**, 014305 (2008).
20. X. Yang, J. Zhou, B. Jones, C. Y. Ng, and W. M. Jackson, "Single-photon vacuum ultraviolet excitation spectroscopy of autoionizing Rydberg states of atomic sulfur", *J. Chem. Phys.* **128**, 084303 (2008).
21. Xi Xing, Mi-Kyung Bahng, Beth Reed, C. S. Lam, Kai-Chung Lau, and C. Y. Ng, "Rovibrationally selected and resolved pulsed field ionization photoelectron study of propyne: Ionization energy and spin-orbit interaction in the propyne cation", *J. Chem. Phys.* **128**, 094311 (2008).
22. Xi Xing, Beth Reed, Mi-Kyung Bahng, S. J. Baek, Peng Wang, and C. Y. Ng, "Infrared-vacuum ultraviolet pulsed field ionization-photoelectron study of CH_3I^+ using a high-resolution infrared laser", *J. Chem. Phys.* **128**, 104306 (2008).
23. Jing Wang, Yuyang Li, Taichang Zhang, Zhenyu Tian, Bin Yang, Kuiwen Zhang, Fei Qi, Aiguo Zhu, Zhifeng Cui, and C. Y. Ng, "Interstellar Enols Are Formed in Plasma Discharge of Alcohols", *Astrophys. J.* **676**, 416-419 (2008).
24. Xi Xing, Beth Reed, Mi-Kyung Bahng, and C. Y. Ng, "Infrared-vacuum ultraviolet pulsed field ionization-photoelectron study of C_2H_4^+ using a high-resolution infrared laser", *J. Phys. Chem. A* **112**, 2572-2578 (2008).
25. Mizuki Oku, Yu Hou, Xi Xing, Beth Reed, Hong Xu, C. Y. Ng, Kiyoshi Nishizawa, Keijiro Ohshimo, and Toshinori Suzuki, "3s Rydberg and cationic states of pyrazine studied by photoelectron spectroscopy", *J. Phys. Chem. A* **112**, 2293-2310 (2008).
26. X. Xing, P. Wang, H.-K. Woo, M.-K. Bahng, S.-J. Baek, B. Reed, C. S. Lam, and C. Y. Ng, "Rotationally resolved infrared-vacuum ultraviolet pulsed field ionization-photoelectron depletion method for infrared spectroscopic studies of neutral molecules", *Chem. Phys. Lett.* **455**, 321 (2008).

27. X. Xing, B. Reed, M.-K. Bahng, P. Wang, H.-K. Woo, S.-J. Baek, C. S. Lam, and C. Y. Ng, "High-resolution infrared-vacuum ultraviolet photoion and pulsed field ionization-photoelectron methods for spectroscopic studies of neutrals and cations", *Chinese J. Chem. Phys.* **21**, 193 (2008).
28. Y.-H. Chiu and R. A. Dressler, D. J. Levandier, C. Houchins, and C. Y. Ng, "Large-Angle Xenon Ion Scattering in Xe-propelled Electrostatic Thrusters: Differential Cross Sections", *J. Phys. D.: Appl. Phys.* **41**, 165503 (2008).
29. C. Chang, Q.-Z. Yin, and C. Y. Ng, "Testing of self-shielding model for early solar nebula with laboratory experiment", *Geochimica et Cosmochimica Acta* **72**, A148, Suppl. 1 (2008).
30. Xi Xing, Peng Wang, Beth Reed, S. J. Baek, and C. Y. Ng, "Infrared-vacuum ultraviolet pulsed field ionization-photoelectron study of CH_3Br^+ ", *J. Phys. Chem. A*, **112**, 9277 (2008).
31. Y. Hou, H.-K. Woo, P. Wang, X. Xing, C. Y. Ng, and K.-C. Lau, "Vacuum ultraviolet pulsed field ionization-photoelectron and infrared-photoinduced Rydberg ionization study of 1,3-butadiene", *J. Chem. Phys.* **129**, 114305 (2008).
32. B. Jones, J. Zhou, L. Yang, and C. Y. Ng, "High-resolution Rydberg tagging time-of-flight measurements of atomic photofragments by single-photon vacuum ultraviolet Laser Excitation", *Rev. Sci. Instrum.*, accepted.
33. B. Reed, C.-S. Lam, Y.-C. Chang, X. Xing, and C. Y. Ng, "A high-resolution photoionization study of ^{56}Fe using vacuum ultraviolet laser", *Astrophys. J.*, accepted.

V.2. Invited lectures acknowledging the support of this AFOSR grant (2006-present)

34 invited lectures (at Universities, Research Institutes, and National and International Conferences and Workshops). See detailed list below.

V.3. Highlights of scientific results and technical developments

Significant scientific and technical accomplishments achieved in this funding period from Jan. 2006 to Nov. 2008 are highlighted below.

V.3.1. Scientific results

Publication 8: This paper presents the methodology developed in our laboratory based on the AFOSR support to generate beams of ions in single quantum states for bimolecular ion-molecule reaction dynamics studies using pulsed-field ionization (PFI) of atoms or molecules in high- n Rydberg states produced by vacuum ultraviolet (VUV) synchrotron or laser photoexcitation. Employing the pseudo-continuum high-resolution VUV synchrotron radiation at the Advanced Light Source (ALS) as the

photoionization source, PFI-photoions (PFI-PIs) in selected rovibrational states have been generated for ion-molecule reaction studies using a fast-ion gate to pass the PFI-PIs at a fixed delay with respect to the detection of the PFI-photoelectrons (PFI-PEs). The fast ion-gate provided by a novel interleaved comb wire gate lens is the key for achieving the optimal signal-to-noise in state-selected ion-molecule collision studies using the VUV synchrotron based PFI-PE-secondary ion coincidence (PFI-PESICO) method. Absolute integral cross sections for state-selected H_2^+ ions ranging from $v^+ = 0$ to 17 in collisions with Ar, Ne and He at controlled translational energies have been obtained by employing the VUV synchrotron based PFI-PESICO scheme. The comparison between PFI-PESICO cross sections for the $\text{H}_2^+ + \text{Ne}$ and $\text{H}_2^+ + \text{He}$ proton-transfer reactions and theoretical cross sections based on quasiclassical trajectory (QCT) calculations and 3D quantum scattering calculations performed on the most recently available *ab initio* potential energy surfaces is highlighted. In both reaction systems, quantum scattering resonances enhance the integral cross sections significantly above QCT predictions at low translational and vibrational energies. At higher energies, the agreement between experiment and QCT calculations is very good. The profile and magnitude of the kinetic energy dependence of the absolute integral cross sections for the $\text{H}_2^+(v^+ = 0-2, N^+ = 1) + \text{He}$ proton transfer reaction unambiguously show that the inclusion of Coriolis coupling is important in quantum dynamics scattering calculations of ion-molecule collisions.

Publication 15: The absolute integral cross sections for the formation of HeH^+ and HeD^+ from the collisions of $\text{HD}^+(v^+, N^+=1) + \text{He}$ have been examined over a broad range of vibrational energy levels $v^+=0-13$ at the center-of-mass collision energies (E_T) of 0.6 and 1.4 eV using the VUV-PFI-PESICO method. The E_T dependencies of the integral cross sections for product HeH^+ and HeD^+ from $\text{HD}^+(v^+=0-4) + \text{He}$ collisions in the E_T range of 0-3 eV have also been measured using the VUV-photoionization-guided-ion beam mass spectrometric technique, in which vibrationally selected $\text{HD}^+(v^+)$ reactant ions were prepared via excitation of selected autoionization resonances of HD. At low total energies, a pronounced isotope effect is observed in absolute integral cross sections for the $\text{HeH}^+ + \text{D}$ and $\text{HeD}^+ + \text{H}$ channels with significant favoring of the deuteron transfer channel. As v^+ is increased in the range of $v^+=0-9$, the integral cross sections of the $\text{HeH}^+ + \text{D}$ channel are found to approach those of HeD^+ . The observed velocity distributions of product HeD^+ and HeH^+ are consistent with an impulsive or spectator-stripping mechanism. Detailed QCT calculations are also presented for $\text{HD}^+(v^+, N^+=1) + \text{He}$ collisions at the same energies of the experiment. The QCT calculations were performed on the most accurate *ab initio* potential energy surface available. If zero-point energy of the reaction products is taken into account, the QCT cross sections for

product HeH^+ and HeD^+ from $\text{HD}^+(\nu^+) + \text{He}$ are found to be significantly lower than the experimental results at E_T values near the reaction thresholds. The agreement between the experimental and QCT cross sections improves with translational energy. Except for prethreshold reactivity, QCT calculations ignoring zero-point energy in the products are generally in good agreement with experimental absolute cross sections. The experimental $\text{HeH}^+/\text{HeD}^+$ branching ratios for the $\text{HD}^+(\nu^+=0-9) + \text{He}$ collisions are also consistent with QCT predictions. The observed isotope effects can be rationalized on the basis of differences in thermochemical thresholds and angular momentum conservation constraints.

Publication 18: Time-dependent wave packet quantum scattering (TWQS) calculations are presented for $\text{HD}^+(\nu^+ = 0-3; N^+ = 1) + \text{He}$ collisions in the E_T range of 0.0-2.0 eV. The present TWQS approach accounts for Coriolis coupling and uses the most accurate *ab initio* potential energy surface. For a fixed total angular momentum, J , the energy dependence of reaction probabilities exhibit quantum resonance structures. The resonances are more pronounced for low J values and for the $\text{HeH}^+ + \text{D}$ channel than for the $\text{HeD}^+ + \text{H}$ channel, and are particularly prominent near the threshold. The quantum effects are no longer discernable in the integral cross sections, which compare closely to QCT calculations conducted on the same potential energy surface. The integral cross sections also compare well to recent state-selected experimental values over the same reactant and translational energy range. Classical impulsive dynamics and steric arguments can account for the significant isotope effect in favor of the deuteron transfer channel observed for $\text{HD}^+(\nu^+ < 3)$ and low translational energies. At higher reactant energies, angular momentum constraints favor the proton-transfer channel, and isotopic differences in the integral cross sections are no longer significant. The integral cross sections as well as the J dependence of partial cross sections exhibit a significant alignment effect in favor of collisions with HD^+ rotational angular momentum vector perpendicular to the Jacobi R coordinate. This effect is most pronounced for the proton-transfer channel at low vibrational and translational energies.

Publication 26: Elastic scatterings between xenon ions and xenon atoms produce ion currents at large angles with respect to the axis of Xe propelled electrostatic thrusters. Differential scattering cross sections are needed to properly predictions off-axis currents that can cause significant material erosion due to sputtering. Guided-ion Beam differential cross section measurements are presented for $\text{Xe}^+ + \text{Xe}$ and $\text{Xe}^{2+} + \text{Xe}$ elastic scattering at laboratory ion energies between 5 and 40 eV per ion charge. For the singly charged system, the experimental absolute differential cross sections are in excellent agreement with classical elastic scattering calculations based on the most recent *ab initio* ion-atom interaction potentials.

The measurements for the doubly charged system are used to derive an approximate effective $\text{Xe}^{2+}\text{-Xe}$ interaction potential. The potentials are used to calculate absolute differential cross sections for both ion charge states at a typical Hall thruster ion energy of 300 eV per unit charge. The differential cross sections for the doubly charged ions are found to be a factor of ≈ 3 smaller than those of the singly charged system at large scattering angles. The importance of doubly charged ions with respect to material erosion is discussed on the basis of known sputtering yields as a function of ion energy for molybdenum and boron nitride. It is concluded that at typical charge-state ratios, doubly charged Xe^{2+} ions generated at elastic scattering angles have sputtering impacts at relatively low ion energies and that the sputtering yields depend very strongly on ion kinetic energy.

V.3.2. Technical developments

In the past funding cycle, we have successfully developed the VUV laser guided ion-beam apparatus for state-selected ion-molecule studies and the VUV laser time-sliced velocity-mapped ion-imaging apparatus for photodissociation studies. Since these apparatuses will be used for the proposed research, their development is described in some detail below.

Development of the VUV laser photoionization guided ion-beam apparatus

In the past three years, we have successfully modified the triple-quadrupole-double-octopole

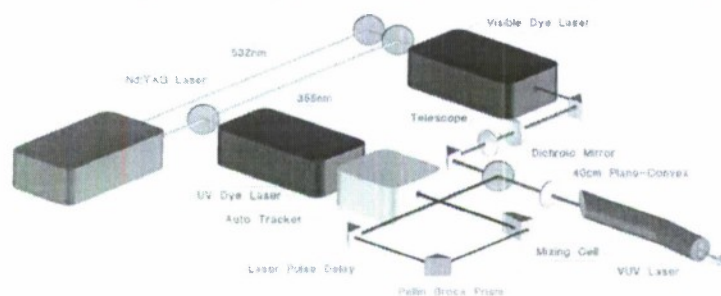


Figure 1. Schematic diagram of the comprehensive VUV laser system, which consists of two Nd:YAG pumped dye lasers and a gas cell or a pulsed jet for four-wave sum- or difference-frequency mixings.

(TQDO) photoionization ion-molecule reaction apparatus in our laboratory into a VUV laser photoionization ion-molecule reaction apparatus, along with many technical improvements as described below. The main effort for the upgrade involves the replacement of the VUV discharge lamp system by a comprehensive tunable VUV laser system, such that the VUV laser photoionization and pulsed field ionization techniques can be used for the preparation of state-selected reactant ions. Figure 1 shows the layout of the VUV laser system used in our laboratory, which consists of an injection seeded Nd:YAG pumped laser (repetition rate = 15 Hz, pulsed energies = 1.6 J at 1064 nm, 550 mJ at 532 nm, and 325 mJ at 355 nm), two dye lasers [one UV and one visible, optical bandwidth of 0.03 cm^{-1}], and a nonlinear frequency mixing chamber, where the

rare gases (Ar, Kr, and Xe) or Hg vapor can be used in the form of a pulsed jet (or gas cell) as the nonlinear media for frequency mixings. The output of UV dye laser is obtained by frequency doubling and/or mixing using BBO crystals and is fixed at ν_1 to match the two-photon UV-resonance of a rare gas or Hg. The ν_2 output of the visible dye laser is tunable.

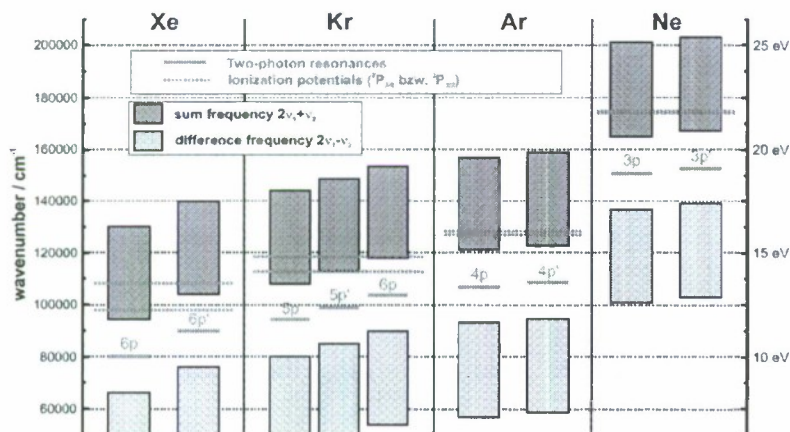


Figure 2. Four-wave sum- and difference-frequency mixing schemes using the rare gases. By utilizing the np and np' (n = for Ar, 5 and 6 for Kr, and 6 for Xe) states, the combined sum-frequency (marked as blue) and difference-frequency (marked by yellow) range cover the VUV range of 6.5-19.5 eV.

Figure 2 shows the general four-wave mixing schemes in rare gases, which utilizing the np and np' ($n=4$ for Ar, 5 and 6 for Kr, and 6 for Xe) levels as the $2\nu_1$ resonance states, where the sum-frequency ($2\nu_1 + \nu_2$) and difference-frequency ($2\nu_1 - \nu_2$) ranges are marked in blue and yellow, respectively. We find that the UV and visible dye laser tunable ranges can be extended by Raman frequency shifting in H_2 (D_2) and CH_4 , and thus, coherent VUV laser radiation with optical band-width of 0.12 cm^{-1} (FWHM) can be generated in the VUV range of 7.0-19.5 eV without any gaps. For a VUV laser equipped with a windowless VUV monochromator for separating the VUV sum- or difference-frequency from the fundamental frequencies ν_1 and ν_2 , the obtainable VUV laser pulse energy is $\approx 1\text{ }\mu\text{J}$. By using a Kr gas cell for nonlinear mixing and a MgF_2 convex lens instead of a monochromator to separate the ν_1 and ν_2 frequencies from the VUV difference-frequency, we have measured a VUV pulsed energy of $\approx 10\text{ }\mu\text{J}$ or a photon intensity of $>10^{14}$ photons/s for a 30 Hz laser as compared to that of 10^9 - 10^{10} photon/s at the high-resolution (resolution ≈ 1 - 5 cm^{-1} , FWHM) VUV synchrotron source of the Chemical Dynamics Beamline at the ALS. This increase in VUV laser intensity is critically important for the success of the VUV-PFI scheme for the preparation of state-selected ions. For VUV wavelengths shorter than $1050\text{ }\text{\AA}$ (absorption cutoff of LiF), a convex lens can no longer be used to separate the VUV from fundamental frequencies. Recently, we have overcome this problem by intersecting the two dye laser beams at a slight angle onto a rare gas jet, such that the VUV beams of sum- and difference-frequencies would emerge in directions different from those of the fundamental UV and visible laser beams. This arrangement,

which allows the selection of the VUV beam of interest by using a slit without a monochromator or a convex lens, has been successfully implemented in our laboratory.

For absolute total state-selected cross section measurements using the VUV laser PFI-photoion (PFI-PI) scheme, we have simplified the TQDO apparatus by eliminating the middle quadrupole mass filter (QMF), resulting in the quadrupole-octopole-octopole-quadrupole (QOOQ) arrangement as shown in Fig. 3. In addition to the original reaction gas cell 1(10), we have installed reaction gas cell 2 (11) for charge transfer studies. Since reaction gas cell 2 is situated between rf-octopole 1 (9) and rf-octopole 2 (12), a small dc field can be applied between octopoles 1 and 2 to extract slow charge transfer product ions for detection. The dual octopole arrangement also allows product ion kinetic energy analyses by time-of-flight (TOF) measurements.

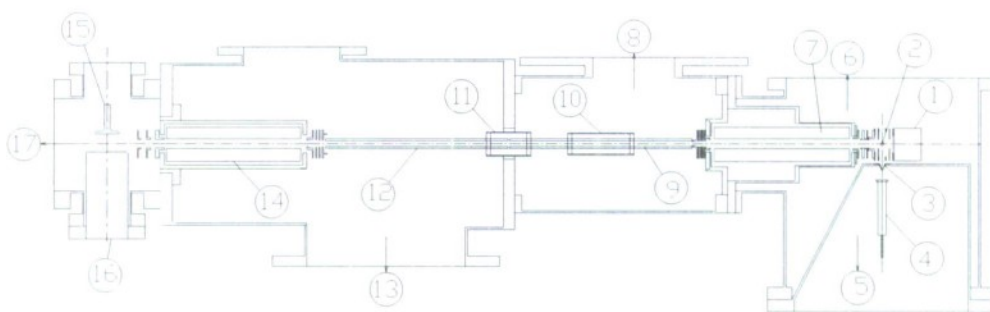


Figure 3. Schematic diagram for the VUV laser quadrupole-octopole-octopole-quadrupole (QOOQ) apparatus. (1) MCP detector for ions or electrons, (2) photoionization center, (3) skimmer, (4) pulsed nozzle, (5) beam source chamber (to 5000 L/s diffusion pump (PD)), (6) photoionization chamber (to 500 L/s turbomolecular pump (TMP)), (7) reactant quadrupole mass filter (QMF), (8) reaction chamber 1 (to 500 L/s TMP), (9) radio-frequency (rf)-octopole 1, (10) reaction gas cell 1, (11) reaction gas cell 2, (12) rf-octopole 2, (13) reaction chamber 2 (to 5000 L/s DP), (14) product QMF, (15) ion target, (16) MCP detector, (17) Daly ion detector (to 500 L/s TMP).

Furthermore, we have implemented a genetic algorithm to maximize the ion transmission of the QOOQ apparatus. In the past, for each cross section measurement at a given $E_{c.m.}$, individual ion lenses were manually adjusted to optimize the ion transmission. Using the genetic algorithm, the voltage settings of ion lenses can be automatically optimized by a personal computer to give the highest reactant and product ion transmissions. We have also replaced the scintillation-phototube assembly of the Daly ion detector with a set of MCP detectors, resulting in lowering the ion background to ≤ 0.1 counts/s. Since the MCP detector is insensitive to minor scattered light from UV and visible lasers, this modification allows the introduction of the laser source into the reaction gas cell along the central axis of the octopole and quadrupole assembly for

photoionization sampling of atoms or radicals prepared in the gas cell. Knowing that the optimal ion trapping rf-frequency depends on the ion mass, we have also constructed a broad band rf impedance matching driver for the octal ion guides, such that the rf amplitude can remain constant in the full rf range of 1.8-30 MHz. A fast rf on/off switch has also been installed, allowing the rf power to the octopole to be turned off for 1 to 10 ms at the repetition rate of the VUV laser. This procedure is important for eliminating ion background due to secondary reactions of trapped ions in the gas cell.

The groups of Softly and Anderson have previously examined the rotational energy effects in the $\text{H}_2^+(\nu^+=0, N^+=0-4) + \text{H}_2$ and the $\text{NO}^+(\nu^+=0, N^+) + \text{C}_2\text{H}_5\text{I}$ reactions by using two-photon PFI-PI or MATI techniques to prepare the state-selected reactant ions. The two-color UV-UV-PFI-PI schemes for the preparation of state-selected ions are limited to the existence of stable UV intermediate states, whereas the VUV-PFI-PI scheme does not suffer from this limitation, and is generally applicable to all states resolved in the PFI-PE spectrum of a molecular ion. For PFI-PI detection using pulsed VUV lasers, PFI-PIs formed from PFI of high- n Rydberg species must be separated from prompt background ions using a dc-separation field and an appropriate time delay between the application of the VUV laser pulse and the pulsed PFI electric field. The time delay requirement demands long lifetimes for the high- n Rydberg states. Schlag and co-workers have demonstrated that using a small scrambling electric field during the laser excitation to promote the Stark mixing to high orbital angular momentum l -states from low l -states originally formed in laser excitation can significantly lengthen the Rydberg lifetimes and thus enhance the PFI-PI signal. We have constructed a circuit to generate an exponentially decaying pulse train (period=20 ns) as show in Fig. 4(a). By varying the delay of firing the VUV laser with respect to the initiation of this pulse train, the amplitude of the scrambling pulse can be optimized to give the highest PFI-PI signal. As an example, we show in Fig. 4(b) the comparison of the TOF spectra that resolved the prompt ion and PFI-PI peaks for $\text{NO}^+(\text{X}, \nu^+=1)$ recorded with (blue) and without (red) the scrambling field. A 3-fold increase in the PFI-PI intensity is observed when the scrambling field is switched on and the VUV frequency is fixed at the transition of the Q-branch of $\text{NO}^+(\text{X}, \nu^+=1)$. For some rotational transitions of $\text{NO}^+(\text{X}, \nu^+=1)$, a 10-fold enhancement was observed.

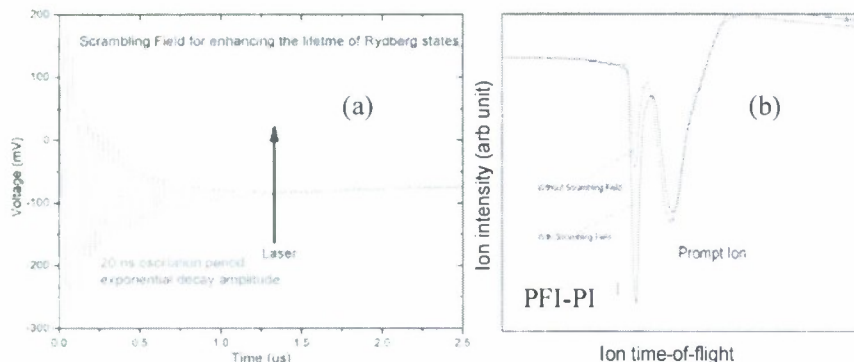


Figure 4. (a) Application of a scrambling field to stabilize high- n Rydberg states prepared by VUV excitation. (b) Oscilloscope traces of the TOF spectra, resolving the PFI-PI and prompt ion peaks. The spectra with and without the scrambling field are in blue and red, respectively.

In order to use the PFI-PIs formed for state-selected ion-molecule reaction studies, it is necessary to reject the prompt ions. Figure 5(a) shows the voltage settings applied to the repeller plates V_1 and V_2 at the photoionization region for separating the PFI-PIs (blue ion cloud) from the prompt ions (red ion cloud). The apertures of both repeller lenses V_1 and V_2 are covered by high transmission gold grids. By applying an electric pulse (height = -30 V, width = 2 μ s) to V_1 after the PFI-PIs pass V_2 , but before the prompt ions exit the photoionization region, we find that the prompt ions are rejected and only the PFI-PIs are detected by the MCP detector [see the TOF spectrum on the right side of Fig. 5(b)].

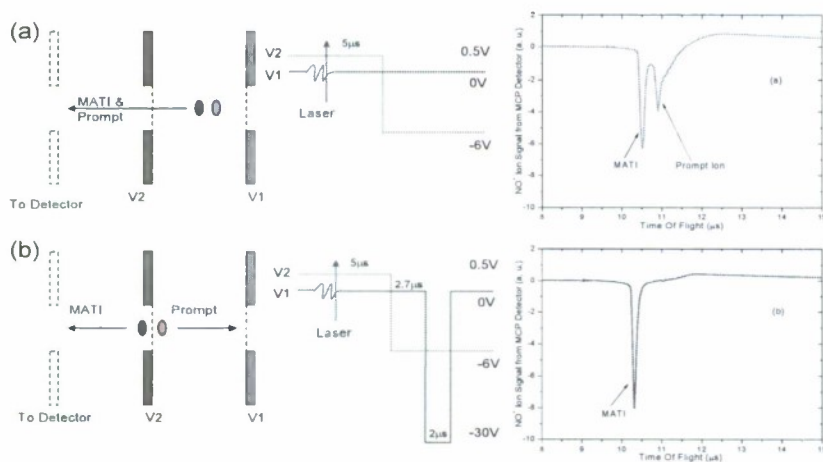


Figure 5. (a) TOF spectrum (on the right side) showing the NO^+ PFI-PI and prompt NO^+ peaks. (b) TOF spectrum (on the right side) showing the NO^+ PFI-PI peak after the prompt NO^+ background peak was blocked by a pulsed electric field applied to the repeller V_1 . The corresponding voltage settings used are shown on the left side of (a) and (b).

Figure 6 compares the rotationally resolved PFI-PE and PFI-PI spectra of $\text{NO}^+(X; v^+=1)$, together with the simulated spectrum. Due to the higher PFI voltage used in the PFI-PI measurement, the energy resolution for the PFI-PI spectrum is lower than that of the PFI-PE spectrum. Nevertheless, the low J^+ states are still clearly resolved. We find that a PFI-PI intensity of $1.5 \times 10^4/\text{s}$ can be obtained for NO^+ in $v^+=0, 1$, or 2 state. As a demonstration experiment, we have obtained absolute total charge transfer (CT) cross sections for the $\text{NO}^+(X; v^+=0-2) + \text{C}_6\text{H}_6$ (CH_3I) collisions at $E_{\text{c.m.}}=0.4-5$ eV (see Fig. 7). As expected, the C_6H_6^+ and CH_3I^+ CT cross sections are sensitive to the $\text{NO}^+(v^+)$ state; but not the $E_{\text{c.m.}}$. The observed CH_3I^+ cross sections for $\text{NO}^+(X; v^+=0, 1$ and 2) are $\approx 1, 10$, and 20 \AA^2 , respectively, which are consistent with the fact that

$IE[NO \rightarrow NO^+(v^+=2)] = 9.84 \text{ eV} > IE[NO \rightarrow NO^+(v^+=1)] = 9.55 \text{ eV} \approx IE(CH_3I) = 9.54 \text{ eV} > NO^+(v^+=0) = 9.26$. Since $IE[NO \rightarrow NO^+(v^+ = 0, 1 \text{ and } 2)] > IE(C_6H_6) = 9.24 \text{ eV}$, the $C_6H_6^+$ cross sections for $v^+ = 0-2$ are all very high ($>60 \text{ \AA}^2$).

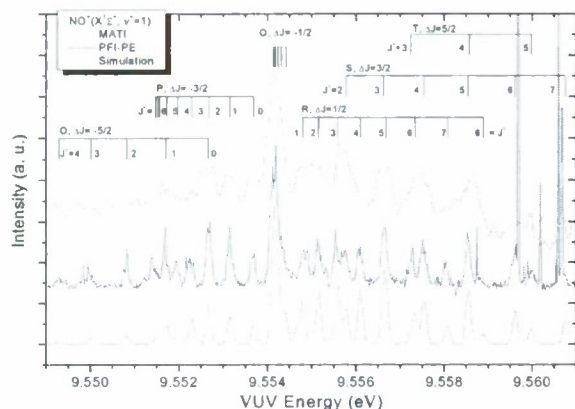


Figure 6. Rotational-resolved PFI-PE (middle) and MATI (upper) along with the simulated (bottom) spectra for $NO^+(X, v^+=1, J^+) \leftarrow NO(X, v''=0, J'')$. Rotational temperature = 50 K.

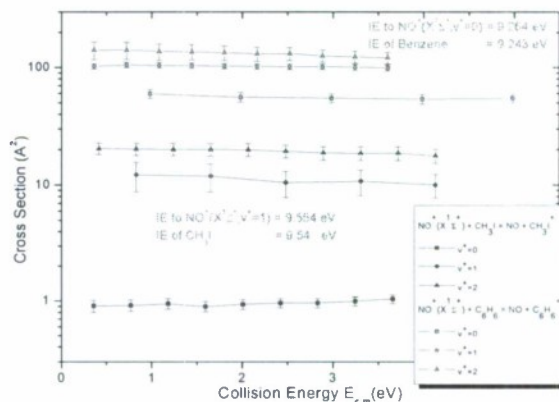
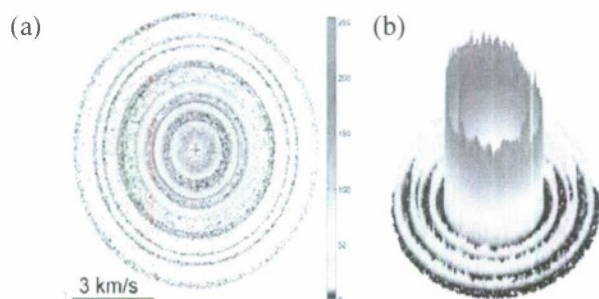
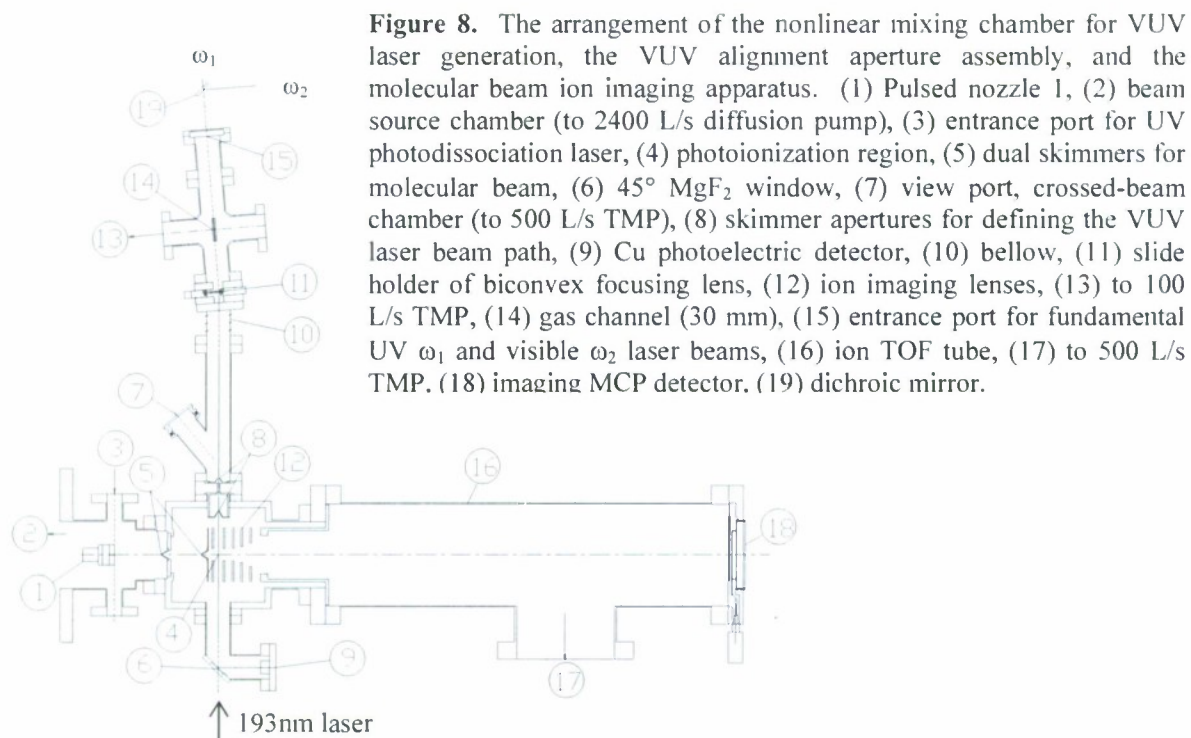


Figure 7. $C_6H_6^+$ (red) and CH_3I^+ (blue) CT cross sections for the $NO^+(X; v^+=0-2) + C_6H_6$ (CH_3I) collisions at $E_{c.m.}=0.4-5 \text{ eV}$. (■) $v^+=0$; (●) $v^+=1$; and (▲) $v^+=2$.

The success of this experiment represents a significant advance in ion-molecule reaction studies because it demonstrates that rovibrational-state-selected ion-molecule collision experiments can be made in individual laboratories using VUV lasers. Since the preparation of PFI-PIs is triggered by the VUV laser pulse, their collisions with neutral reactants in the form of a pulsed beam can be synchronized easily. The beam-beam arrangement will eliminate the Doppler broadening effect in using neutral reactants in a thermal gas cell, and thus significantly improve the kinetic energy resolution for ion-neutral collision studies. Many pulsed neutral atomic and radical beam sources based on pulsed UV laser photodissociation are well established. The establishment of the VUV-PFI-PI QOOQ apparatus will allow absolute cross section measurements of state-selected ion-atom or radical reactions, which is essentially a new field.

Development of the VUV laser time-sliced velocity-mapped ion-imaging apparatus

We have developed a state-of-the-art VUV laser molecular beam ion imaging apparatus for photodissociation and photoionization studies (Publications 2, 19, and 21). Figure 8 shows the coupling of the nonlinear mixing chamber for VUV laser generation with the ion imaging apparatus. To illustrate the high velocity resolution ($\Delta v/v = 1.5\%$), we depict in Figs. 9(a) and 9(b) the respective 2-D and 3-D ion velocity-mapped image of O^+ fragments formed in the photodissociation of vibrationally excited $O_2^+(X; v^+)$ produced by resonance-enhanced multiphoton ionization (REMPI) at 225.000 nm. The analysis shows that the rings resolved in Fig. 9(a) correspond to the photodissociation of excited $O_2^+(X)$ in different v^+ states.



In VUV-photoionization and UV-photodissociation studies, VUV laser radiation generated by four-wave difference-frequency mixing schemes in a pulsed Kr (or Xe) gas stream in the gas channel (14) are selected and focused by the offset-axis biconvex MgF₂ lens (11) before entering the PD/PI region (4) of the ion imaging apparatus. The 193 nm photodissociation laser is counter propagated relative to the VUV laser beam and enters the PD/PI region through the 45°-tilted MgF₂ window (6).

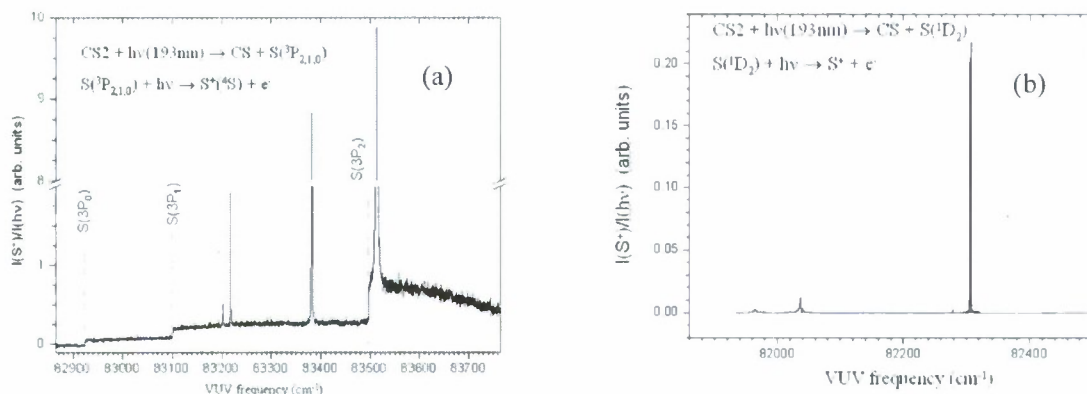


Figure 10. (a) PIE spectra for $S(^3P_{2,1,0})$ and (b) $S(^1D_2)$ formed in 193nm photodissociation of CS_2 .

The atoms in specific states produced in photodissociation can be monitored and characterized by VUV photoionization. As an example, we show in Figs. 10(a) and 10(b) the VUV laser PIE spectra of nascent $S(^3P_{2,1,0})$ and $S(^1D)$ formed by the 193nm photodissociation of CS_2 . The IEs of $S(^3P_0)$, $S(^3P_1)$, and $S(^3P_0)$ are marked by sharp steps in the spectrum. The PIE spectrum for $S(^1D_2)$ is recorded at VUV frequencies below the IE of $S(^3P_0)$ and is found to exhibit only sharp autoionizing resonances.

By parking the VUV laser at a sharp autoionizing resonance of Fig. 10(b), we have obtained the time-sliced velocity-mapped for the $\text{CS}_2 + h\nu(193\text{nm}) \rightarrow \text{CS}(v) + S(^1D_2)$ reaction [Fig. 11(a)], which is different from that for the $\text{CS}_2 + h\nu(193\text{nm}) \rightarrow \text{CS}(v) + S(^3P_{2,1,0})$ reactions observed by

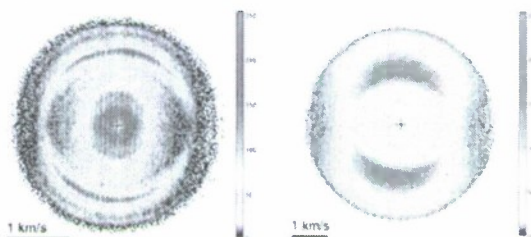


Figure 11. Time-sliced velocity-mapped ion images of S^+ formed by VUV photoionization of $S(^3P_{2,1,0})$ (right image) and $S(^1D)$ (left image).

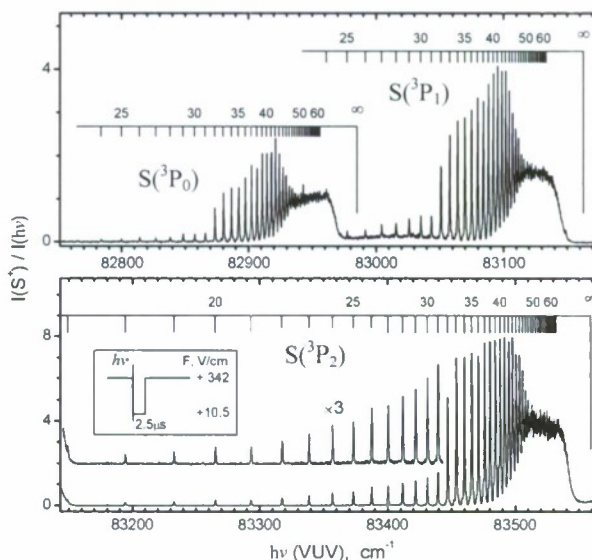


Figure 12. VUV-PFI-PI bands for $S(^3P_0)$, $S(^3P_1)$, and $S(^3P_2)$ in the frequency range of $82,750$ – $83,570 \text{ cm}^{-1}$. The inset illustrates the electric field pulse used for the PFI-PI measurement. The firing of the VUV laser was delay by 150 ns with respect to the falling edge of the electric field pulse.

parking the VUV laser at the steps of the PIE curve of Fig. 10(a).⁵¹ Based on the imaging measurement, we also conclude that the autoionizing lines resolved in Fig. 10(a) originate from $S(^1D)$.

The most interesting result is that we have been able to obtain the VUV laser PFI-PI electronic bands for $S(^3P_0)$, $S(^3P_1)$, and $S(^3P_2)$ (Fig. 12). The relative intensities observed for these bands allows the determination of the branching ratios for these fine structure states, $S(^3P_0) : S(^3P_1) : S(^3P_2) = 1.00 : 1.54 : 3.55$, produced by photodissociation of CS_2 at 193 nm. Furthermore, the analysis of the Rydberg series resolved in Fig. 12 has provided more precise IE values for $S(^3P_0)$ [$82,985.43 \pm 0.05 \text{ cm}^{-1}$], $S(^3P_1)$ [$83,162.94 \pm 0.05 \text{ cm}^{-1}$], and $S(^3P_2)$ [$83,559.04 \pm 0.05 \text{ cm}^{-1}$].

We have also observed the VUV-PFI-PI bands for the $CS_2^+(^2\Pi_{3/2})$ and $CS_2^+(^2\Pi_{1/2})$ states with excellent intensities, indicating that it may be possible to perform UV laser photodissociation studies of state-selected ions by the velocity ion imaging techniques. Furthermore, the VUV laser PFI-PI experiment on $S(^3P_{2,1,0})$ also points to the feasibility of performing high-resolution Rydberg tagging TOF measurements on S and other atoms.

VI. Personnel Supported:

- | | | |
|----|-------------------------|------------------------|
| 1. | Professor Cheuk-Yiu Ng: | Principal investigator |
| 2. | Dr. Chao Chang | Postdoctoral associate |
| 3. | Dr. Jingang Zhou | Postdoctoral associate |
| 4. | Dr. X.-N. Tang | Ph.D. student |
| 5. | Dr. Yu Hou | Ph.D. student |
| 6. | Mr. Cassidy Houchins | Ph.D. student |
| 7. | Ms. Hong Xu | Ph.D. student |

VII. Interactions/Transitions:

VII.1. Invited talks at workshops, conferences, and seminars (2006-present)

1. C. Y. Ng, "Two-color Infrared-Vacuum Laser Ultraviolet photoion-photoelectron studies", Gordon Research Conference on "*Photoions, Photoionization and Photo-detachment*", Santa Yuez Valley Mariot, Buellton, CA, Jan 31-Feb. 3, 2006.

2. "State-Selected Ion Molecule Reactions", Chemical Dynamics Beamline Review, Lawrence Berkeley Laboratory, Berkeley, CA, Feb. 28, 2006. Presented by Rainer A. Dressler.
3. C. Y. Ng, "Benchmarking state-of-the-art ab initio calculations by high-resolution pulsed field ionization photoion-photoelectron measurements", Symposium in honor of Prof. Wai-Kee Li's retirement, Hong Kong, May 13, 2006.
4. C. Y. Ng, "Two-Color Infrared-Vacuum Laser Ultraviolet Photoion-Photoelectron Studies", Overseas Chinese Physics Association Conference, Taipei, Taiwan, June 27-30, 2006.
5. C. Y. Ng, "Frontier in Photoionization and Photoelectron Studies: Recent Development and Future Prospects", National Synchrotron Research Center, Hsinchu, Taiwan. June 29, 2006.
6. C. Y. Ng, "Pulsed Field Ionization Studies of Chemical Energies and Ion Dynamics: Benchmarking state-of-the-art theories", Gordon Research Conference on "Atomic and Molecular Interactions", July 9-14, 2006.
7. C. Y. Ng, "Spectroscopy and Dynamics by High-Resolution Photoion-Photoelectron Studies", Users Meeting, National Synchrotron Radiation Laboratory, Huangshan, Anhui, China. Aug. 16-18, 2006.
8. "State-Selected Ion-Molecule Reaction Dynamics of the Proton Transfer Reactions of $\text{H}_2^+(\text{X}, \text{v}^+)$ [$\text{HD}^+(\text{X}, \text{v}^+)$] + He (Ne)", James Franck Institute, University of Chicago, Chicago, Aug. 22, 2006. (presented by Xiaonan Tang)
9. C. Y. Ng, "Vacuum Ultraviolet Probes: From Fundamental Chemical Dynamics to Reaction Mechanisms of Combustion, catalysis, and Interstellar Chemistry", Workshop on "The UK's 4th Generation Light Source: the next steps", Daresbury Laboratory, Warrington, WA4 4AD, Cheshire, United Kingdom, Friday, Sept. 8, 2006.
10. "State-Selected Ion-Molecule Reaction Dynamics of the Proton Transfer Reactions of $\text{H}_2^+(\text{X}, \text{v}^+)$ [$\text{HD}^+(\text{X}, \text{v}^+)$] + He (Ne)", Sandia National Laboratory, Livermore, CA. Oct. 2, 2006 (presented by Xiaonan Tang)
11. C. Y. Ng, "Two-Color Photoionization-Photoelectron Studies by Combining Infrared and Vacuum Ultraviolet", Workshop on "Multi-color scientific opportunities at CIRCE and the ALS", Advanced Light Source, LBNL, Oct. 9-11, 2006.
12. C. Y. Ng, "Frontier in Photoionization and Photoelectron Studies: Recent Development and Future Prospects", Symposium on "Modern Trends in Molecular Dynamics: From Small Molecules to Biomolecules" in Honor of Prof. Yuan T. Lee's 70th Birthday, Taiwan, Dec. 10-15, 2006.

13. "Spectroscopy of Ions and Neutrons by High-Resolution Two-Color Infrared and Vacuum Ultraviolet Laser Photoionization and Photoelectron Methods", *54th Western Spectroscopy Meeting*, Asilomar, CA, Jan 31-Feb 2, 2007 (presented by Xi Xing).
14. C. Y. Ng, "Spectroscopy of neutrals and ions by two-color infrared-vacuum ultraviolet photoion-photoelectron studies", *Gordon Research Conference on "Gaseous Ions: Structures, Energetics, and Reactions*, Feb. 25-March 2, 2007.
15. C. Y. Ng, "Structures, Energetics, and Reaction Dynamics of Neutrals and Ions by High Resolution Photoionization and Photoelectron Methods", California Institute of Technology, Chemical Physics Seminar, April 24, 2007.
16. C. Y. Ng, "Spectroscopy and Dynamics of Neutrals and Ions by High-Resolution IR-VUV Laser Photoionization and Photoelectron Methods", Department of Chemistry, University of Pacific, Stockton, CA, Sept. 11, 2007.
17. C. Y. Ng, "Spectroscopy and Dynamics of Neutrals and Ions by High-Resolution IR-VUV Laser Photoionization and Photoelectron Methods", *The 10th National Conference of Chemical Reaction Kinetics*, Dalian, China, Sept 21-23, 2007.
18. C. Y. Ng, "Spectroscopy and Dynamics of Neutrals and Ions by High-Resolution IR-VUV Laser Photoionization and Photoelectron Methods", Department of Chemistry, Texas A&M University, Oct. 9, 2007.
19. C. Y. Ng, "Spectroscopy and Dynamics of Neutrals and Ions by High-Resolution IR-VUV Laser Photoionization and Photoelectron Methods", Department of Chemistry, Rice University, Oct. 10, 2007.
20. "Spectroscopy of Neutrals and Ions by Two-color photoion-photoelectron of Ions by High-Resolution Two-Color Infrared and Vacuum Ultraviolet Laser Photoionization and Photoelectron Methods", Presented by Xi Xing, Department of Chemistry, Princeton University, Oct. 18, 2007.
21. C. Y. Ng, "Rovibrational-State-Selected Ion-Molecule Reactions using the Pulsed-Field Ionization-Photoion Technique", Dalian Institute of Chemical Physics. Oct. 24, 2007.
22. "Spectroscopy of Neutrals and Ions by Two-color photoion-photoelectron of Ions by High-Resolution Two-Color Infrared and Vacuum Ultraviolet Laser Photoionization and Photoelectron Methods", Presented by Xi Xing, Department of Chemistry, University of California, Irvine, Nov. 2, 2007.

23. C. Y. Ng, "Structures, Energetics, and Reaction Dynamics of Neutrals and Ions by High Resolution Photoionization and Photoelectron Methods", Department of Chemistry, University of Hawaii, Manoa, Nov. 19, 2007.
24. C. Y. Ng, "High resolution photoion-photoelectron studies using vacuum ultraviolet and laser sources", *4th National Meeting on Synchrotron Radiation Research*, Nanjing, China, Dec. 2-6, 2007.
25. C. Y. Ng, "Spectroscopy of neutrals and ions by two-color infrared-vacuum ultraviolet photoion-photoelectron studies", Gordon Research Conference on "*Photoions, Photoionization and Photodetachment*", Lucca, Italy, Jan 27-Feb. 1, 2008.
26. C. Y. Ng, "Structures, Energetics, and Reaction Dynamics of Neutrals and Ions by High Resolution Photoionization and Photoelectron Methods", Department of Chemistry, University of Arkansas, Little Rock, March 7, 2008.
27. C. Y. Ng, "Vacuum ultraviolet laser probes of chemical dynamics of aerospace relevance", *AFOSR Contractor Meeting*, May 19-21, 2008.
28. C. Y. Ng, "Determination of Accurate Energetic and Spectroscopic Database for Combustion Radicals and Molecules by High-Resolution Photoion-Photoelectron Methods", Airline Conference Center, Warrenton, Virginia, *DOE Contractors Meeting*, May 27-30, 2008.
29. "Vacuum Ultraviolet Photoionization and Photoelectron Studies of Small Molecules", Air Force Lab., Hanscom, Boston, June 11, 2008 (presented by Beth Reed).
30. C. Y. Ng, "Spectroscopy, Energetics, and Dynamics of Neutrals and Ions by High Resolution Photoionization and Photoelectron Methods", *First Annual workshop of the 10+10 (10 campuses of the University of California +10 universities of China) Alliance Program*, Department of Chemistry, Peking University, June 9, 2008.
31. "High resolution pulsed-field ionization for spectroscopy and ion-molecule reaction dynamics", Air Force Lab., Hanscom, Boston, June 17, 2008 (presented by Cassidy Houschins).
32. "High resolution pulsed-field ionization for spectroscopy and ion-molecule reaction dynamics", Naval Research Lab., Washington, D. C., June 20, 2008 (presented by Cassidy Houschins).
33. C. Y. Ng, "Opening Remarks and Concluding Remarks", *The 5th National Synchrotron Radiation Meeting on Soft X-ray and Vacuum Ultraviolet: Techniques and Applications*, Kunming, China, Aug. 1 and 2, 2008.

34. C. Y. Ng, "Chemical Dynamics by VUV photoionization Probes", ACS symposium on *Spectroscopic Probes of Chemical Dynamics in Gaseous and Condensed Phase*, Philadelphia, Aug. 17-21, 2008.

VII.2. Interactions

This project represents a collaborative project between our group at UC Davis and Dr. Y.-H. Chiu, Dr. James Dodd at the Hanscom Air Force Research laboratory. Dr. Albert Viggiano of the Hanscom Air Force Research Laboratory is also interested to collaborate with us to measure the vibrational energy distributions of product O_2^+ , NO^+ , and N_2^+ formed in the reactions of $O^+ + O_2$ (N_2), which are the most reactions occurring in planetary atmospheres.

VII.3. Transitions

The differential scattering cross sections for the $Xe^+ + Xe$ charge transfer reaction are important experimental data, which can be used to properly predict off-axis currents in electrostatic thrusters that can cause significant material erosion due to sputtering. The thermochemical data obtained by our group based on VUV photoion and photoelectron measurements have been used by the "Active Thermochemical Table" project (project leader: Dr. Branko Ruscic) of the Argonne National Laboratory.

VIII. New Discoveries:

None

IX. Honors/Awards:

Lifetime achievement honors

- 2008 Siu Lien Ling Wong Visiting Fellow, Chung Chi College,
The Chinese University of Hong Kong
- 2005 Elected Fellow, American Association for Advancement of Science
- 2001 Distinguished Professor, UC Davis
- 1998 Alexander von Humboldt Senior Scientist Award
- 1997 Senior Fellow, Japanese Society for the Promotion of Science
- 1996 Distinguished Professor of Liberal Arts and Sciences, Iowa State University

- 1994 Iowa Regents Award for Faculty Excellence
- 1993 Elected Fellow, American Physical Society
- 1985 Honorary Professor of Chemistry, Zhengzhou University, China
- 1982 Camille and Henry Dreyfus Teacher-Scholar
- 1981 Alfred P. Sloan Foundation Fellow